Journal of Marine Research, 50, 207–228, 1992

Water characteristics, mixing and circulation in the Bay of Bengal during southwest monsoon

by V. S. N. Murty, [1], Y. V. B. Sarma,[1] D. P. Rao[1] and C. S. Murty[1]

ABSTRACT

Influence of the freshwater influx, the wind forcing and the Indian Ocean monsoon drift current on the property distributions and the circulation in the Bay of Bengal during southwest monsoon has been quantified. At the head of the Bay, waters of low salinity, affected by the freshwater influx, occupy the upper 90 m water column. The isohaline 34.0×10^{-3} separating these waters from those of underlying saline waters shoals southward gradually and outcrops around 14N, 10N and 6N in the western, central and southeastern regions of the Bay respectively. The wind-stress-curl-induced upwelling effect is confined to depth limits of 50–100 m as is supported by a band of cold (24°–19°C) water in the central Bay. In the southern and central regions of the Bay, the monsoon drift current feeds the large scale cyclonic gyre apart from maintaining the northward flowing boundary current in the eastern Bay. A warm (27°–23°C), saline ($35.0–35.2 \times 10^{-3}$) watermass is advected northeastward along with the monsoon drift current into the Bay up to 14N at the depth limits of 50–100 m. Below this depth, in the western Bay a well-defined southward flow in the form of a boundary current is documented. Intense vertical mixing is inferred at the zones of salinity fronts in the depth limits of 40–100 m and also at deeper depths (> 2200 m) and elsewhere lateral mixing is predominant.

1. Introduction

The earliest oceanographic investigations in the Bay of Bengal began with the studies of Sewell (1925, 1932). Subsequent studies were confined to the slope and shelf regions of the western Bay (Anon, 1954, 1958; Ramasastry and Balaramamurty, 1957; Varadachari, 1961). R & D efforts based on International Indian Ocean Expedition (IIOE) data were limited in space and deal with hydrographic characteristics of the waters of parts of the Bay during winter and the accompanying transition period to summer (Anon, 1968; Duing, 1970; Wyrtki, 1971; Rao and Sastry, 1981). The investigators realized the influence of nearly steady winds of the two monsoons (northeast and southwest) on the water circulation in the Bay during the year but could not address it in any quantitative manner. On the same note one could also realize the importance of a major, seasonal external forcing in the form of freshwater influx.

1. National Institute of Oceanography, Dona Paula, Goa - 403 004 India.

It is known that collection of environmental data through conventional/ contemporary means is a monumental task and requires many ships operating. Under steady external forcing, continuity in the collection of data from the area of interest would certainly help in assessing the integral effects of various forcings. Such a data set cannot yield a snapshot of the distribution of heat, salt or water movements.

Until recently, the data available for the summer season (period of the southwest monsoon prevailing from June through September) in the Bay of Bengal were meagre. As a part of the studies on the seasonal and annual variability in the property distributions and circulation of the Bay of Bengal undertaken by the National Institute of Oceanography, general hydrographic surveys were conducted during each season. From one such survey, hydrographic data were collected during the southwest monsoon of 1984 on board ORV *Sagar Kanya* and have been utilized for the present study. In this article, we address the water characteristics, mixing taking place in the interior of the Bay utilizing the density flux function and circulation derived at different horizontal surfaces during the period of southwest monsoon.

For a study of this nature, one would prefer near-synoptic data. Considering the large area of the Bay investigated (stretching from 4N to 20°30'N and extending from 80E to 92E), the survey could only be completed in two phases with a short break in between to facilitate bunkering for the research vessel which has an endurance capacity of only 35 days. Still, the sampling had to be carried out at alternate latitudes while the stations were occupied close to one degree (slightly over the Rossby radius of deformation-90 km) along the latitudes.

During the period of survey, the southwesterly winds of the monsoon were nearly steady barring the short durations over which weather disturbances (Ramasastry *et al.,* 1986) with diverse intensity prevailed. The effects of these weather events on the environmental data collected were assumed to be marginal.

2. Material and methods

The hydrographic data (Fig. 1; Table 1) collected during the southwest monsoon of 1984 on board ORV *Sagar Kanya* using a ME (Meerestechnik Electronik) Sonde CTD system were utilized in the present study. Apparently spurious values, believably the observational errors, were checked prior to drawing any conclusion from the distribution patterns constituting such data sets. Conventional data processing methods were followed and outlined in Murty (1990). Typical charts showing the distribution of T, S and σ_t at select horizontal surfaces and vertical sections were presented. Topological maps (abbreviated as topomaps) showing the thickness of the surface homogeneous layer (THL) and the depths of three isothermal (25°C, 20°C and 13°C) surfaces representing the upper, middle and lower thermocline and one isohaline (34.0×10^{-3}) surface were also included. To deduce the currents and the

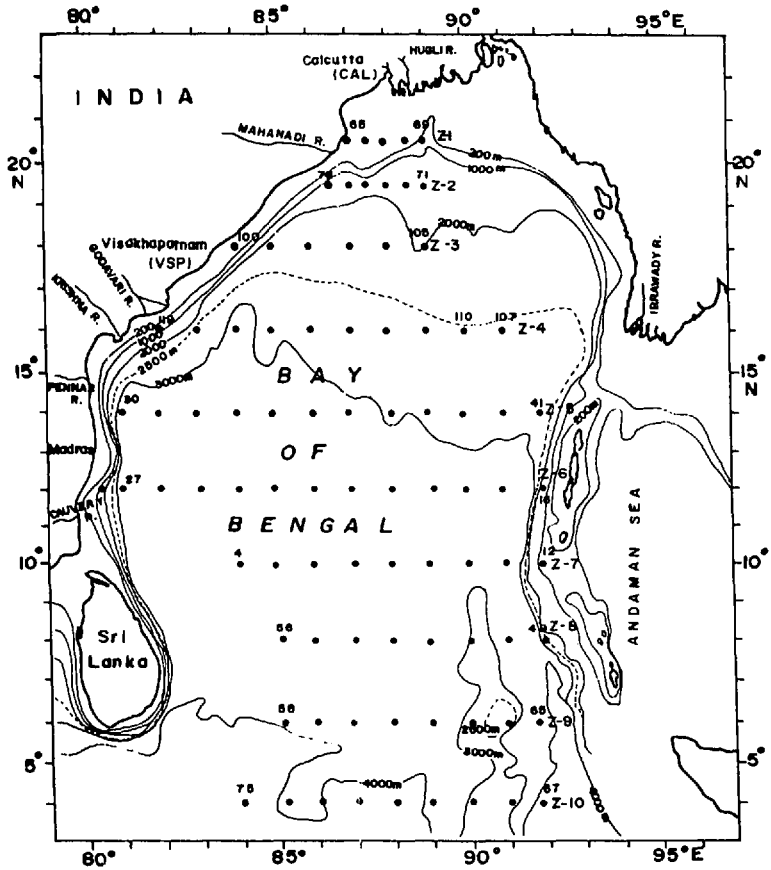

Figure 1. Station locations (●) together with the bathymetry of the Bay of Bengal. The major rivers along the boundary of the Bay are shown. Numerals at the dots are the assigned station serial numbers.

associated circulation patterns, the dynamic method (Sverdrup *et al.*, 1942; Pond and Pickard, 1983) was employed. Three reference levels—500 db, 1000 db and 2500 db—were chosen to delineate the extent of freshwater influx, wind forcing and deep thermohaline effects. The specific volume anomaly was extrapolated following Sverdrup *et al.* (1942) and Fomin (1964) for the data collected from stations with sampling depths shallower than the depth of reference level. The density flux function (τ), with its surface orthogonal to potential density surface in the T-S plane, is an indicator of nature of mixing (lateral and vertical) in conjunction with density (Veronis, 1972) and has been computed from the polynomial expression:

$$\tau = \sum_{i=1}^{6} \sum_{j=1}^{6} A_{ij} (\theta - 10)^{i-1} (S - 35)^{j-1}$$

Table 1. Details of hydrographic stations occupied in the Bay of Bengal on board ORV *Sagar Kanya* during SW monsoon of 1984.

Station (Numbers)	Section	Lat. (°N)	Long. (°E) from to	Dates of survey
		Phase I		
65–69	Z-1	20.5	87–89	29–30/7
71–76	Z-2	19.5	89–86	30–31/7
100–105	Z-3	18	84–89	10–12/8
107 & 110–119	Z-4	16	91–81	13–18/8
		Phase II		
30–41	Z-5	14	81–92	14–24/9
16–28	Z-6	12	92–80.5	9–13/9
4–12	Z-7	10	84–92	4–9/9
49–56	Z-8	8	92–85	26–29/9
58–65	Z-9	6	85–92	30/9–2/10
67–75	Z-10	4	92–84	3–6/10

Numbers of stations and sections are shown in Figure 1.

where θ is the potential temperature and S the salinity. The coefficients of linear fit A_{ij} were taken from Veronis (1972). Since the isolines of this function are, by definition, orthogonal to the isopycnals in the T-S diagram (Veronis, 1972), a change in the function τ along any isopycnal indicates lateral mixing and a change in σ_t along any isoline of τ suggests mixing across isopycnic surfaces, i.e. vertical mixing (p. 158; Mamayev, 1975). Veronis (1972) mentions possible ways of interpreting the distribution of density flux function to identify the nature of mixing.

3. Results

A cursory examination of the property distributions enables division of the study area into northern (north of 15N), central (between 15N and 9N) and southern (south of 9N) regions. In the following, the spatial variation of T, S and σ_t at the sea surface, 50 m, 100 m and 500 m and along 18N, 12N and 6N zonal sections is presented.

a. Temperature. The sea surface temperature (SST) decreases from 30.0°C in the northwestern Bay to 27.5°C in the southwestern Bay (Fig. 2a). At 50 m, a band of cold (<24°C) water (marked by arrow in Fig. 2b) oriented in a SW-NE direction is present between 8N and 18N. West of this cold water band, alternate warm (28°C) and cold (24°C) water cells prevail while east of it the temperature increases gradually with the isotherms nearly parallel to the axis of the band. The distribution is more organized at 100 m depth (Fig. 2c). The axis of cold water seen at 50 m shifts westward (toward the Indian coast, Figs. 2b & 2c) at this depth and becomes less prominent at 500 m depth (Fig. 2d).

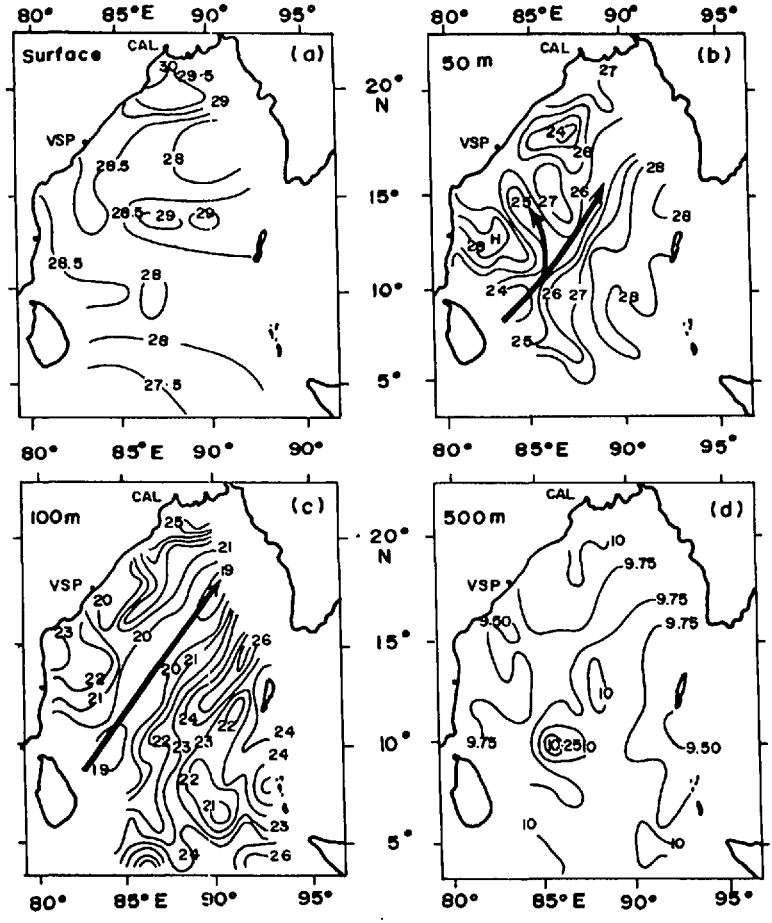

Figure 2. Horizontal maps of temperature (°C) at (a) Surface, (b) 50 m, (c) 100 m and (d) 500 m. (The arrow indicates the axis of cold water band.)

The vertical distribution of temperature reveals the development of surface homogeneous layer with an increase in its thickness towards southern Bay (Figs. 3a–c). In the northern and central Bay, the presence of the cold water is evident in the upper 100 m between 86E and 87E along 18N and between 86E and 88E along 12N and 6N sections. These waters could be identified in the form of fronts with cross-front gradients of 1.3×10^{-2} °C/km at subsurface depths from 40 m to 100 m.

b. Salinity. The surface salinity increases from 16.0×10^{-3} in the north to 35.0×10^{-3} in the southwestern part (Fig. 4a) with waters of salinity below 34.0×10^{-3} occupying a larger area of the Bay. At 50 m (Fig. 4b), a tongue of high ($> 35.0 \times 10^{-3}$) salinity water is seen in the central Bay with its axis (shown by solid arrow) lying 200 km to the east of the cold water axis (shown by dashed arrow) in the southern Bay and

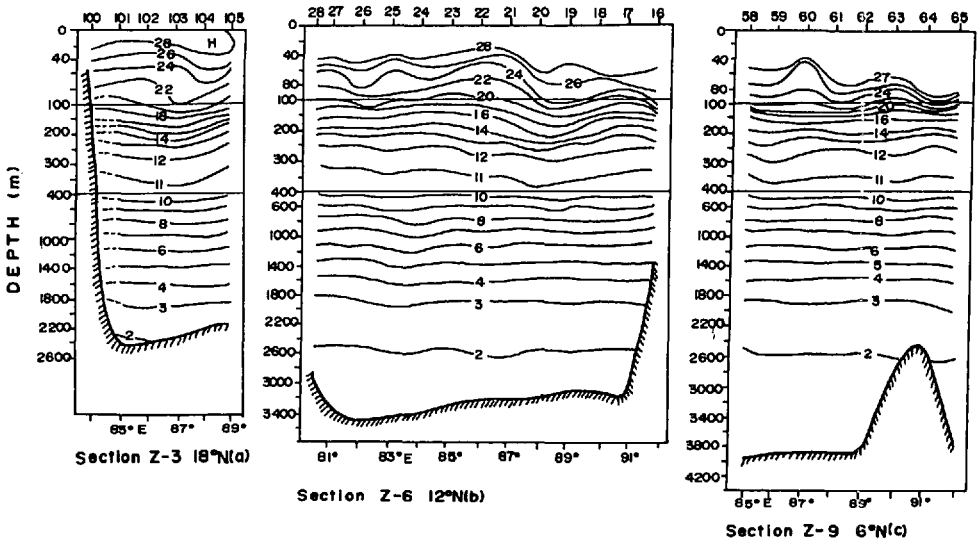

Figure 3. Vertical sections of temperature (°C) along (a) 18N, (b) 12N and (c) 6N.

about 100 km in the central Bay. In the eastern Bay the core of the high salinity water follows the 27°C isotherm. This feature is seen up to a depth of 100 m (Fig. 4c). At 500 m (Fig. 4d), a relatively saline ($>35.08 \times 10^{-3}$) water encompassed by 35.08×10^{-3} isohaline (shown by $\leftrightarrow$) appears in the central Bay. The distribution broadly presents alternate zonal bands of high and low salinity.

The vertical distribution of salinity shows low saline waters (Figs. 5a–c) near the sea surface influenced by uneven spreading of freshwater. One can notice the pockets of high ($>35.2 \times 10^{-3}$) saline water in the depth zone of 50–100 m in the central and southern regions. Subsurface (40–100 m) salinity fronts occur along 18N between 86E and 87E (Fig. 5a) and along 12N between 87E and 90E (Fig. 5b). Along 6N, the salinity front is present in the eastern Bay from surface to 100 m depth (Fig. 5c). A layer of intermediate high ($>35.1 \times 10^{-3}$) salinity water (stippled area in Figs. 5a–c) is present between 200 and 600 m in the south Bay (Fig. 5c) which loses its salinity marginally towards the north (Figs. 5c to 5a).

c. Sigma-t. The density distribution at the sea surface follows that of salinity and exhibits an increase from 10.0 σ_t in the north Bay to 22.5 σ_t in the southwestern Bay (Fig. 6a). At 50 m (Fig. 6b), both temperature and salinity contribute to the density variation while below 50 m depth, the distribution follows the temperature pattern. A tongue of high density water with its axis (shown by arrow in Figs. 6b & 6c) oriented in a SW-NE direction is noticed in the central Bay at depths of 50 m and 100 m. At 500 m the density variation is small and its distribution is characterized by many cells of low and high density (Fig. 6d).

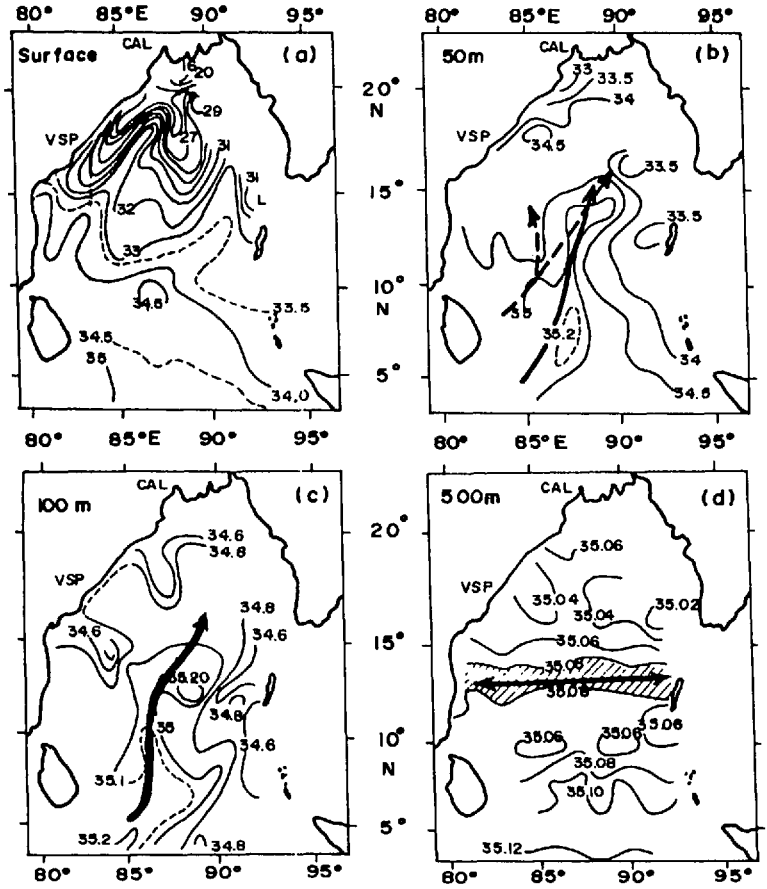

Figure 4. Horizontal maps of salinity ($\times 10^{-3}$) at (a) Surface, (b) 50 m, (c) 100 m and (d) 500 m. (The solid arrow indicates the axis of the high salinity tongue. The dashed arrow in (b) represents the axis of cold water band as at Figure 2b.)

d. Density flux function (τ). The distribution of τ is presented for the upper 200 m water column along the zonal (19°30'N to 4N) sections (Figs. 7 a–i). Its distribution below 200 m is not changed appreciably from one section to the other. Lower values of τ (about 3.0), resulting from the waters of lower salinity, prevails near the sea surface in the north Bay and higher τ (about 7.0) in the south Bay (along 4N) where it is uniform in the upper 100 m. Pockets of subsurface higher τ, coinciding with the subsurface high salinity pockets (Figs. 5b & 5c), are present in the depth limits of 40–100 m following the 23.0 and 24.0 isopycnals (shown by broken lines in Figs. 7a–i) along sections 6N to 14N (Figs. 7h to 7b). Within this depth range, the function τ decreases eastward along the isopycnals and the isolines 6.5 and 7.0 of τ intersect the isopycnals towards eastern Bay along the sections 6N to 14N. Above 40 m and below 100 m, the isolines of τ and σ_t are parallel each other. This is more obvious from

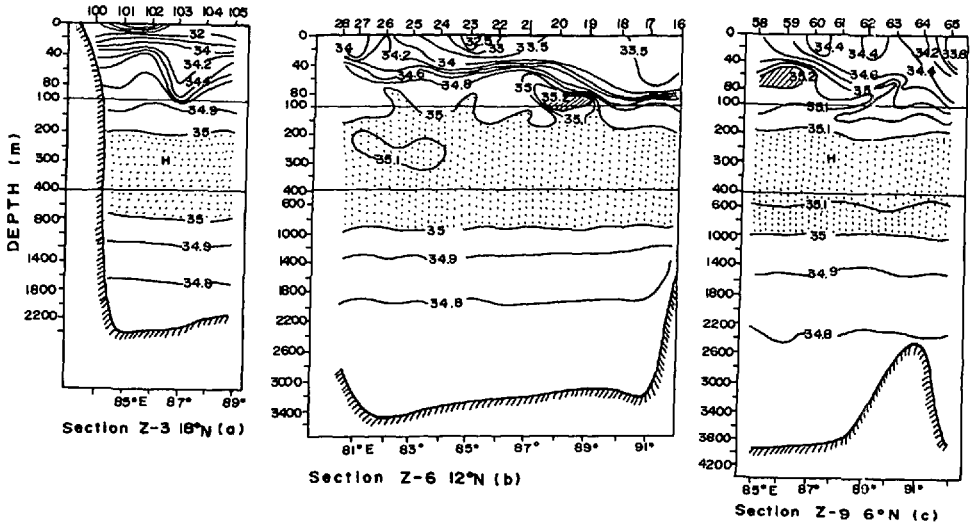

Figure 5. Vertical sections of salinity ($\times 10^{-3}$) along (a) 18N, (b) 12N and (c) 6N.

Figure 8 showing the meridional distribution of τ along 88E. One can also notice the intersection of the isolines of τ and isopycnals at subsurface depths in the depth limits of 40–100 m and at deeper depths (> 2200 m).

Our interpretation is that intense vertical mixing takes place in the Bay of Bengal at deeper depths and at subsurface depths (40–100 m) and elsewhere lateral (isopycnal) mixing is the predominant process. Vertical mixing at subsurface depths occurs at the boundary of the subsurface high salinity pockets and the relatively lower salinity waters in the eastern Bay. This boundary coincides with the temperature and salinity fronts identified at subsurface depths along the zonal sections (Fig. 9). The temperature fronts are noticed only along 12N and 14N sections. The zones of these fronts and the vertical mixing (shaded blocks) are depicted in Figure 9 together with their depth limits.

e. Circulation. The geopotential anomaly computed relative to each of the three different pressure surfaces of 500 db, 1000 db and 2500 db (Murty, 1990) shows insignificant differences in the magnitudes below water depths of 500 m (1 dyn. cm for 500 m layer between 500 db and 1000 db and for 1500 m layer between 1000 db and 2500 db).

The surface circulation (Figs. 10 a–c) is characterized by a great cyclonic gyre covering the Bay south of 15N. The eastward flow near 5N is the Indian Ocean monsoon drift current (Düing, 1970; Wyrtki, 1973), also known as the Indian monsoon current (Molinari *et al.,* 1990), which turns northwestward between 90E and 92E and merges with the flows from west of the Andaman Islands at 10N. Surrounding this cyclonic gyre, are anticyclonic cells influenced by freshwater from the rivers such as the Irrawady in the east; the Ganges and the Brahmaputra in the

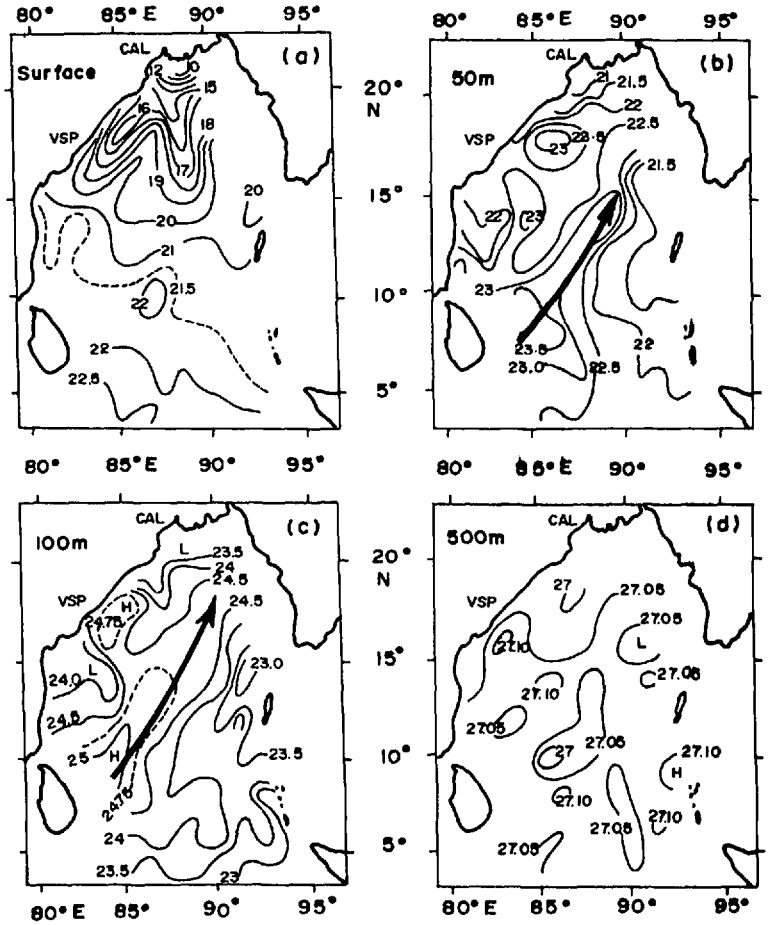

Figure 6. Horizontal maps of σ_t (C.G.S. units) at (a) Surface, (b) 50 m, (c) 100 m and (d) 500 m. (The arrow indicates the axis of dense water.)

north; the Krishna and the Godavari in the western Bay. In the southeastern Bay, one notices a well developed northward flowing eastern boundary current west of the Nicobar Islands. In the western Bay, a cyclonic cell prevails between 15N and 18N. It is interesting to note that the northeastward flow of this cyclonic cell is in the direction of prevailing southwesterly winds in the offshore areas.

The flow pattern at 100 m depth (Fig. 11) presents a northeastward line of flow in the central Bay. The flow is predominantly anticyclonic on the east of this line of flow. In the western Bay, the southward directed flow (as a boundary current) exhibits meandering nature. It envelops two anticyclonic eddies with a cyclonic cell sandwiched in between around 16N. The monsoon drift current in the southern Bay is less distinguishable. Nonetheless, the eastern boundary current west of 92E persists.

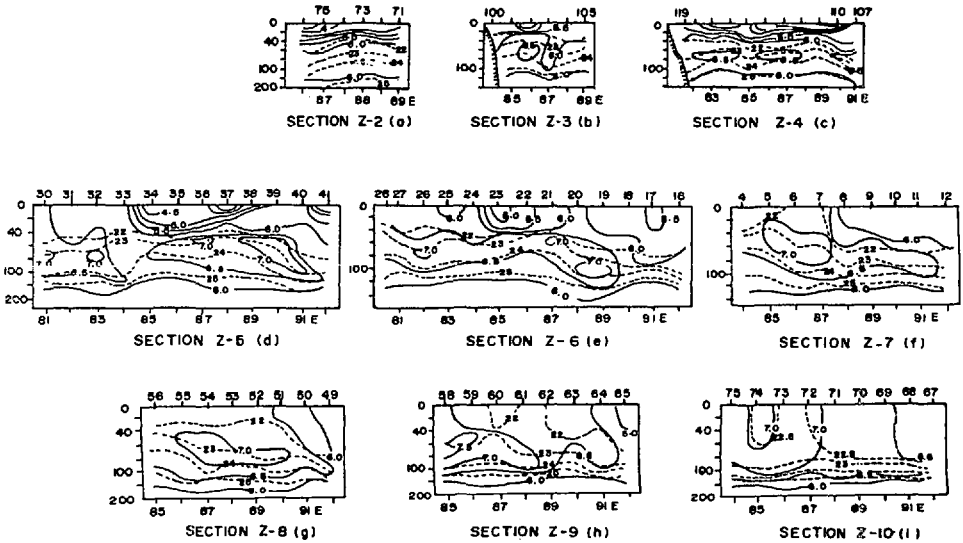

Figure 7. Vertical sections of density flux function (solid lines) and σ_t (broken lines) along the zonal sections from Z-2 to Z-10.

The vertical structure of the currents (Figs. 12a–c) in the upper 1000 m (obtained relative to 1000 db surface) across the zonal (18N, 12N and 6N) sections reveals the presence of alternating northward (hatched areas) and southward (non-hatched areas) currents. A broad northward current with speed exceeding 10 cm/s at the sea surface prevails across 18N (Fig. 12a). The northward flow is associated with relatively saline waters while the southward flow brings waters of low salinity from the north Bay. Across 12N (Fig. 12b), the strong (>40 cm/s) northward current between 87E and 88E transports high salinity waters followed by a southward current (20 cm/s) between 88E and 91E bringing relatively less saline waters towards south. The weak (<10 cm/s) northward current between 85E and 87E corresponds to the cold water band at this latitude. There is also a strong (50 cm/s) subsurface southward flowing current near the Indian coast. Across 6N (Fig. 12c), the northward current (20 cm/s) between 85E and 86E is associated with high ($>35.2 \times 10^{-3}$) salinity waters of the monsoon drift current. A southward current with its core (>40 cm/s) situated at 150 m between 90E and 91E prevails over the 90E ridge (see Fig. 1). Northward currents prevail on either side of the ridge with relatively strong (>40 cm/s) flows between 91E and 92E in the form of an eastern boundary current. This northward current, on the contrary, is associated with relatively less salinity waters.

4. Discussion

Bay of Bengal receives 50×10^3 m^3/s of freshwater by way of surface discharge annually (Varkey, 1986). This does not include the contribution received at the sea

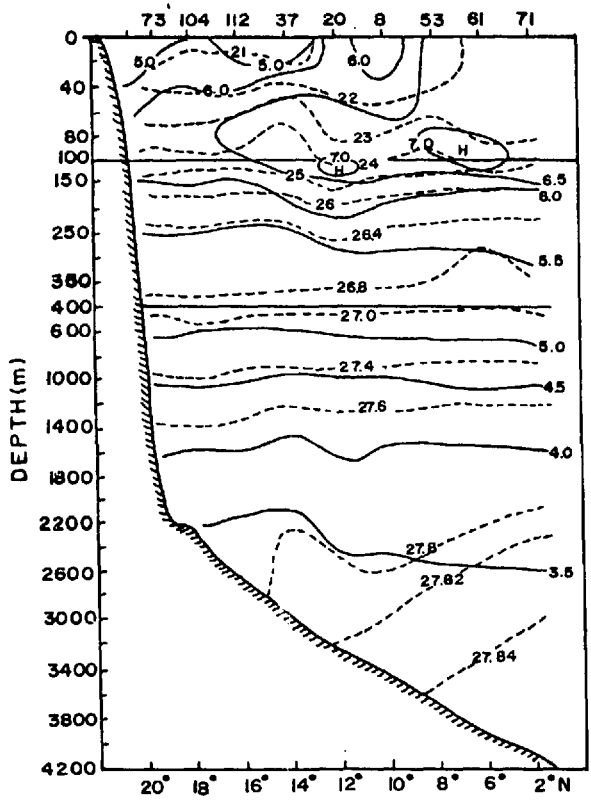

Figure 8. Vertical section of density flux function (solid lines) and σ_t (broken lines) along 88E.

surface in the form of direct precipitation during southwest monsoon period (June–September). If this quantity of freshwater spreads uniformly over the surface of the Bay, having an area of 2.2×10^{12} m^2, a water level rise by 70 cm results. However, the distribution of freshwater is largely controlled by the density driven flows (circulatory or otherwise) and prevailing winds over the Bay.

The distribution of salinity at the sea surface and at depths above 50 m indicates the occurrence of a salinity front across 10N and oriented in a SE-NW direction separating less saline ($<34.0 \times 10^{-3}$) waters on its north from the relatively saline ($>34.0 \times 10^{-3}$) waters on its south. Waters with much less salinity, predominantly seen near the riverine outlets, get advected by the prevailing density driven flows (influenced partly by wind stress). This could be seen from the patches of low salinity water at the sea surface along the zonal sections located over the rising subsurface high salinity waters (Figs. 5a–c). This observation enables one to reason that their movement is governed by the density driven (geostrophic) currents and not by local winds. Similar observation in the Caribbean Sea was made by Metcalf (1968) while examining the hydrographic characteristics and currents off the northeastern coast of

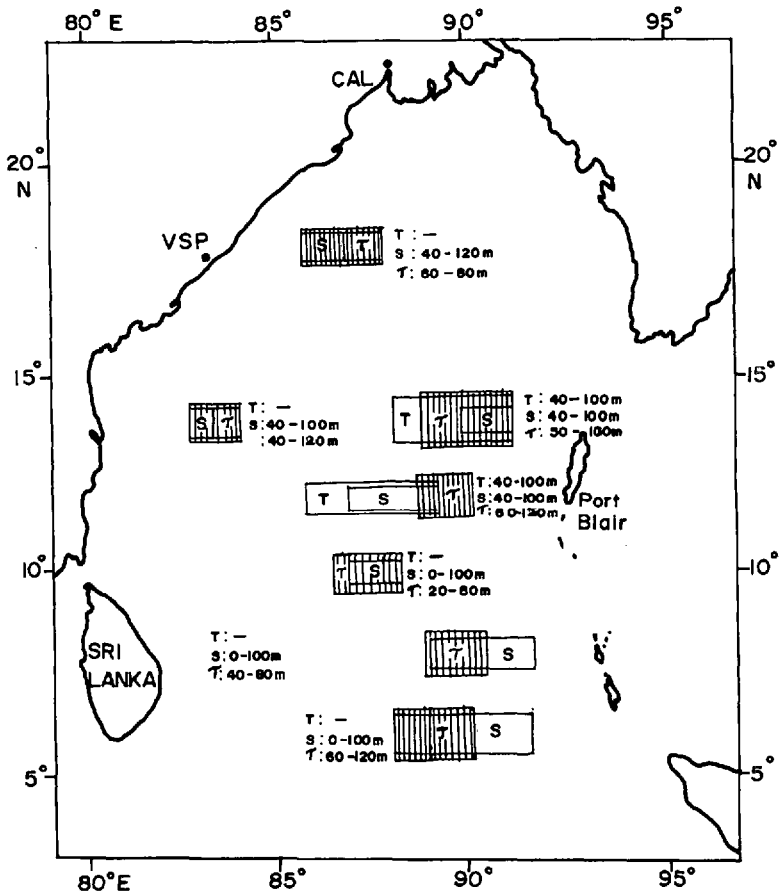

Figure 9. Zones of temperature fronts (T block) and salinity fronts (S block) and vertical mixing (τ, shaded block) together with their depth limits.

South America. The isohaline 34.0×10^{-3} has been considered as a cut-off limit in space for the influence of freshwater discharges into the Bay. This is clearly noticed from the depth of occurrence of this isohaline (Fig. 13) in the region of interest. The ridge structure (shown by arrow in Fig. 13) suggests that the depth of influence of low salinity waters is limited to 40 m in the central Bay (up to 12N). Its influence penetrates up to 90 m at the head of the Bay and the Andaman and Nicobar Islands. In the western Bay, the low salinity water influence is restricted to a maximum of 50 m. The depth contour labelled zero (shown by broken line) indicates the southern limit of the influence of low salinity waters. However, the southern region comes under the influence of advection of relatively cold (27.5°C), saline (35.0×10^{-3}) waters of the Arabian Sea via the monsoon drift current. These waters suggest the possibility of advection of cold, upwelled waters from the southeastern Arabian Sea (off the Kerala coast along the west coast of India) during southwest monsoon

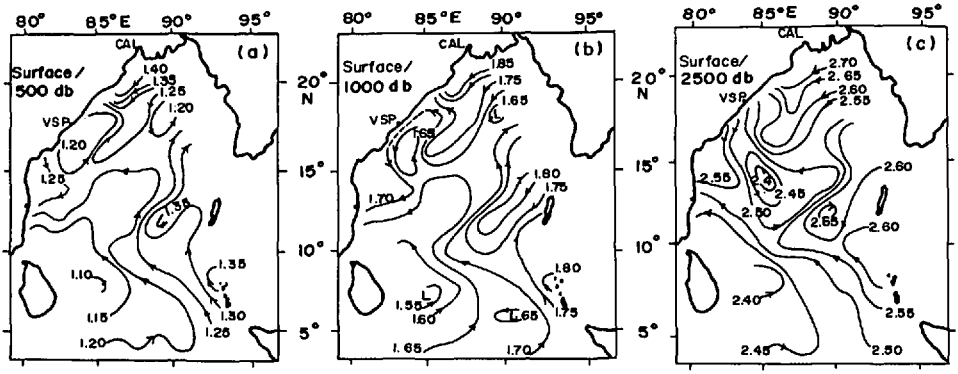

Figure 10. Dynamic topography (dyn.m) at the sea surface relative to (a) 500 db, (b) 1000 db and (c) 2500 db surfaces.

towards southern Bay though higher evaporation (Hastenrath and Lamb, 1979a) and upwelling processes (McCreary, 1990) are suggested for the lower (< 27.5°C) surface temperatures in the southern Bay during southwest monsoon.

The presence of warm (28°–29°C) water around 14N (Fig. 2a), west of the Andaman Islands, during summer season has not been documented earlier. However, based on other surveys by the Institute during early winter season of 1983, the presence of warm waters in this area has been reported (Suryanarayana *et al.*, 1992).

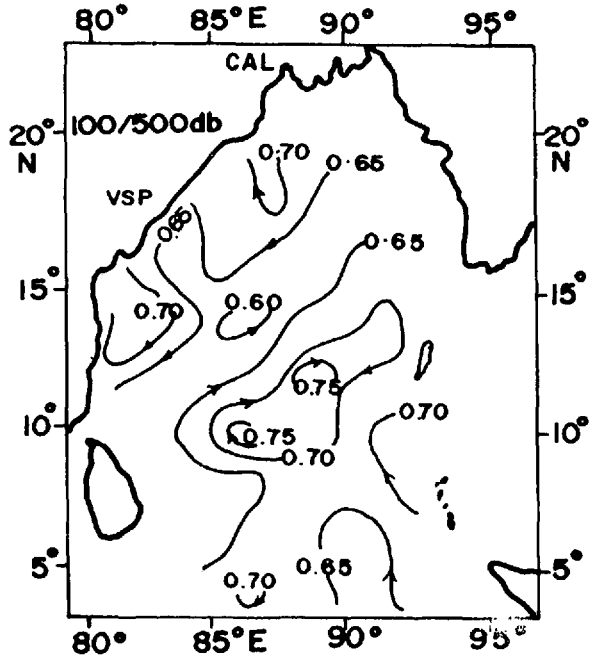

Figure 11. Dynamic topography (dyn.m) at 100 m relative to 500 db surface.

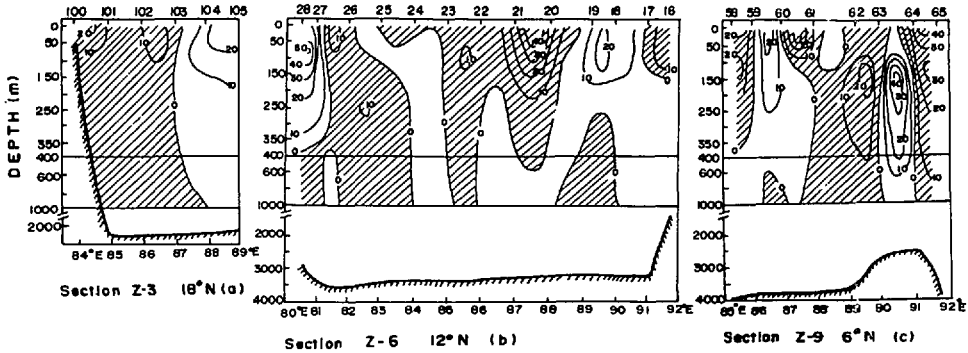

Figure 12. Vertical structure of the geostrophic currents (cm/s) along (a) 18N, (b) 12N and (c) 6N. (Hatching indicates northerly flow. Please note the change in the depth scale for bottom topography.)

This suggests that the presence of warm waters west of the Andaman Islands is a quasi-permanent feature.

The topo-maps of the THL and the isothermal (25°C, 20°C and 13°C) surfaces also indicate a ridge structure (shown by arrow in Figs. 14a–d) in the central region of the Bay. The axis of the ridge structure remains invariant for the topo-maps of the THL,

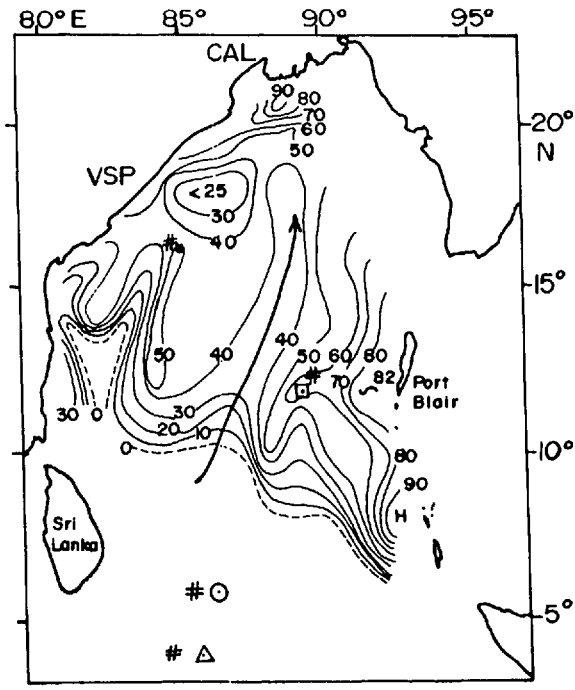

Figure 13. Topology of the 34.0 × 10^{-3} isohaline. (Numbers indicate depth in meters. The arrow indicates the axis of the ridge structure. The station locations of the *T-S* curves presented are also depicted.)

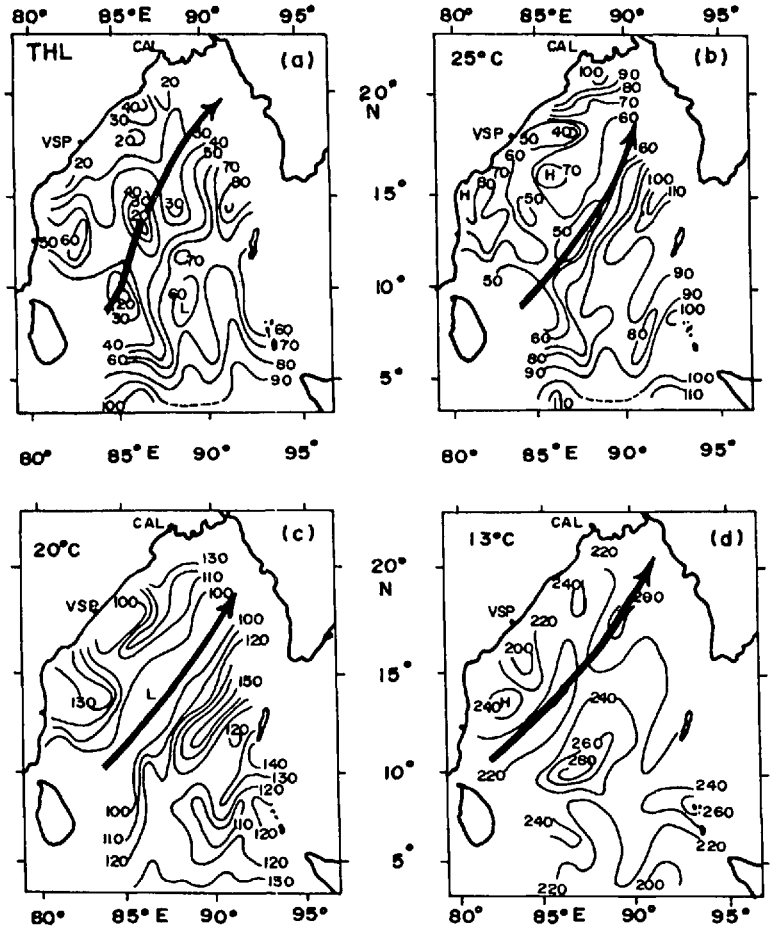

Figure 14. Topological maps of (a) the thickness of the surface homogeneous layer (THL) and (b–d) the isothermal surfaces. (Numbers indicate depth in meters. The arrow denotes the axis of the ridge structure.)

25°C and 20°C isothermal surfaces. However, it exhibits a westward shift by about 100 km towards the western boundary of the Bay on the topo-map of 13°C isothermal surface. The shift on the southwestern end is more evident than that at the other end. The trough structure, however, extends southward as one moves from the topological maps of 25°C to 20°C isotherms.

To understand the development of the ridge structure or the associated cold water band, the distribution of wind stress curl and the associated vertical motion at the base of the Ekman layer for September (Fig. 15a–b) only have been considered since most of the present hydrographic data from the central and southern regions of the Bay were obtained during this period.

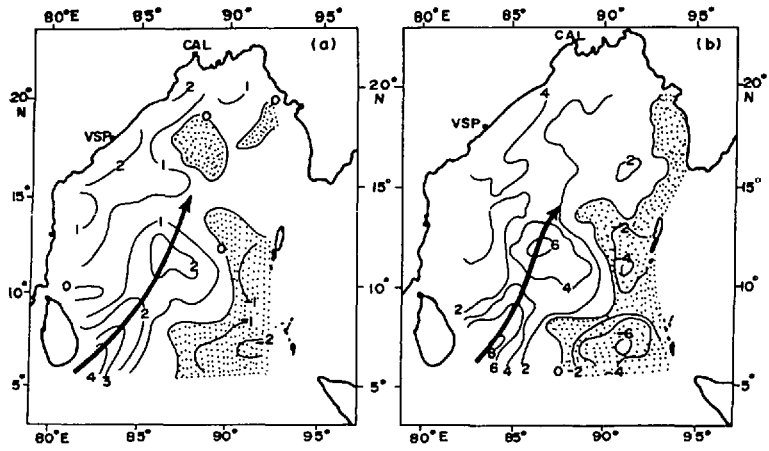

Figure 15. Fields of (a) wind stress curl (10^{-7} N/m^3) and (b) vertical velocity (10^{-6} m/s) at the base of the Ekman layer for September (After Babu, 1987). (The stippled area in each figure indicates the negative curl and downward vertical motion. The arrow in each figure is the axis of positive curl and upward vertical motion.)

During this month, the large and positive curl (2×10^{-7} N/m^3) over the central region (Fig. 15a), with its axis (shown by arrow) oriented in a SW-NE direction, induces upward vertical motion with a magnitude of 6×10^{-6} m/s (Fig. 15b) at the base of the Ekman layer. As a result, the thickness of the surface homogeneous layer (THL) reduces and the isotherms (25°C to 13°C) shoal upwards along the above axis (Figs. 14a–d). Consequent to this, a ridge structure on the topological maps and cold water band (oriented in a SW-NE direction) on horizontal surfaces result.

The positive curl decreases in magnitude towards western Bay and increases near the Indian coast north of 15N. Correspondingly, the THL and the isothermal surfaces deepen initially towards west of the ridge and shoal upward near the Indian coast between 15N and 19N. This shoaling is due to the prevailing relatively high upward vertical motion (4×10^{-6} m/s) in this region from July onwards (Hastenrath and Lamb, 1979b; Babu, 1987).

The negative curl over the eastern and southern regions favors downwelling of magnitude 4–6 $\times 10^{-6}$ m/s and hence to a large THL towards east and south of the ridge structure (Fig. 14a). The topo-maps of the isotherms also indicate a trough structure towards east and south of it (Figs. 14b–d).

In the northern Bay, the lesser (< 30 m) THL is due to the upward motion induced by the positive curl during July–August and aided by the presence of warm (> 29°C) and less ($< 20 \times 10^{-3}$) saline surface waters. Interestingly, the topo-maps of the isothermal and 34.0×10^{-3} isohaline surfaces deepen in this region.

Though all the topo-maps exhibit similar ridge structure over the central Bay, changes in its width, however, prevail. Under the influence of the positive wind stress curl, one expects an increase in the width of the ridge structure. This is evident from

13°C topo-map to 20°C topo-map (Figs. 14 d & c) coinciding with depths of 200 m and 100 m. This feature is less pronounced from 20°C topo-map to 25°C topo-map (Figs. 14 c & b) with a decrease in the width of the ridge from 100 m to 50 m. This underlines the relative importance of Ekman processes over that of wind stress curl in the upper 100 m.

The prevailing southwesterly winds give rise to southeastward Ekman transport at the sea surface. This transport from the western Bay to the region influenced by the positive curl over the central Bay leads to the decrease in the width of the cold water band as observed at 50 m depth offsetting the effect of the curl induced upwelling. The eastward extension of the tongue-like pattern in the temperature distribution at 50 m depth (Fig. 2b) from the western Bay supports the above. Largely, the upper 50 m thick layer is influenced by the freshwaters.

The presence of cold waters in the upper layers of the central Bay decreases the dynamic height and leads to cyclonic flows (Figs. 10a–c). The magnitudes of these flows (Fig. 12b) are low (<10 cm/s). The major axis of the large cyclonic gyre encompassing the Bay south of 15N in the upper 50 m coincides with the axis of this cold water. The cyclonic gyre is influenced largely by the monsoon drift current (Figs. 10a–b) from the south. This monsoon drift current brings warm (27°–23°C) and high ($35.0–35.2 \times 10^{-3}$) salinity waters (Fig. 2b and Fig. 4b) into Bay with the tongue of high salinity at 50–100 m depth defining the cyclonic gyre clearly. The quasi-geostrophic model studies (p. 227; Marchuk and Sarkisyan, 1986) also identify the cyclonic gyre in this area. This gyre is surrounded by the anticyclonic cells, influenced by the freshwater influx, limiting the spatial extent of the cyclonic gyre. The intense (>40 cm/s) northward flowing eastern boundary current (west of 92E and south of 10N) west of the Nicobar Islands gets support from the monsoon drift current and transports northward the relatively less salinity (Figs. 4a–c) waters drawn either from the Malacca Strait or from the Andaman Sea.

Similar pattern of surface circulation, characterized by the large cyclonic gyre, persists up to a depth of 50 m. Further below, at 100 m depth, the cyclonic gyre is not distinguishable and an anticyclonic gyre occupies the central Bay. The well defined southward directed flow in the western Bay at 100 m depth, as a boundary current, enveloping two anticyclonic eddies with a cyclonic cell (around 16N) in between could be associated with the return flow of the interior northward directed Sverdrup transport (Babu, 1987). While the prevailing wind stress (directed toward northeast) aids the flows in the central Bay, the freshwater influenced thermohaline flow dominates the northwestern Bay. This is partly due to weakening of the wind forcing west of the major axis (oriented in a SW-NE direction) of southwesterly winds situated over the central Bay (Hastenrath and Lamb, 1979b).

The above warm, high salinity watermass as it advects into the Bay (via the monsoon drift current) at 100 m along 4N shoals up to 75 m depth under the influence of positive curl between 6N and 10N and west of 88E. Further north, this

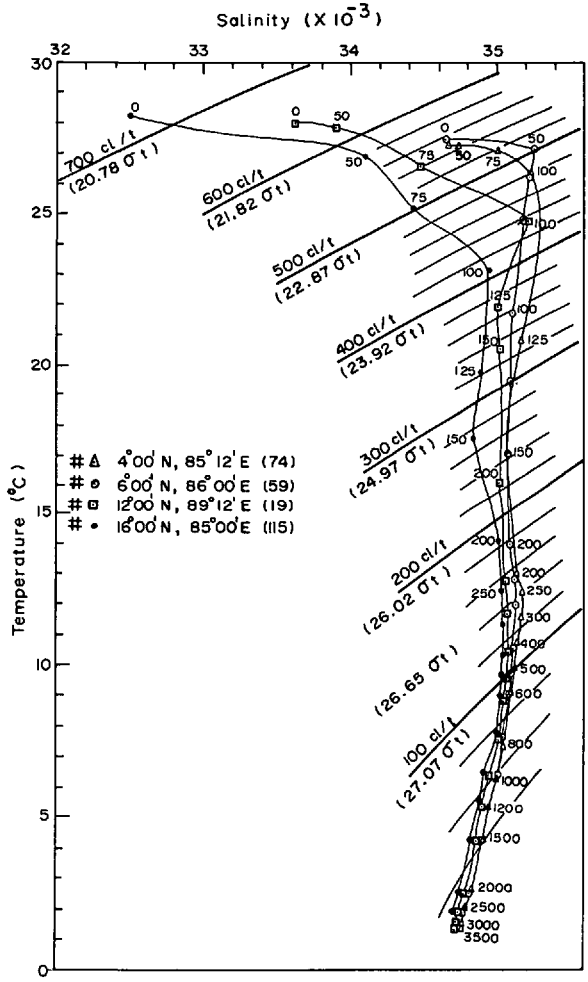

Figure 16. Typical *T-S* curves in the Bay of Bengal during southwest monsoon showing the effect of freshwater influence and presence of the near surface high salinity watermass.

watermass appears at 100 m depth under the influence of negative curl between 10N and 14N and east of 88E. This is evident from the typical *T-S* curves (Fig. 16) representing the northern, central and southern regions (the station locations are depicted in Fig. 13). While the influential effect of freshwater is obvious at the station (16N, 85E) in the northern region, the influence of advection of warm, high salinity watermass is more pronounced at the stations in the southern region. At the station (12N, 89E) in the central region, the effect of both the influences is visualized. From Figure 16, one can also notice the layer of intermediate high (>35.0–35.1×10^{-3}) salinity watermass in the depth zone of 200–900 m between 26.0 and 27.4 isopycnals from south to north Bay with its salinity decreasing marginally towards north. This

nearly-isohaline layer has been suggested as an extension of effect of intrusion of similar isohaline layer (35.7×10^{-3}; between 300 and 900 m) formed in the Arabian Sea due to mixing at the boundary of the high saline Persian Gulf and Red Sea watermasses (Sastry *et al.*, 1985).

Under the influence of curl induced upwelling in the central Bay and the mixing of subsurface high salinity waters with the overlying surface waters of low salinity, waters of relatively less ($< 35.0 \times 10^{-3}$) salinity (compared to core value) are noticed within the area of the cold water band. The core of the high salinity watermass is seen in the warm water area about 100–200 km away from the cold water axis. Consequently, sharp spatial gradients occur in temperature and salinity leading to the development of frontal structures at depths of 50 to 100 m. Vertical mixing becomes predominant at these fronts (Fig. 9). Stable conditions developed due to overlying less saline waters contribute to low vertical mixing in the upper 50 m water column. It is worth mentioning that the vertical mixing inferred at deeper depths (> 2200 m) through the density flux function is in good agreement with the estimated upward vertical flow (with a mean velocity of 2.0×10^{-6} m/s) from depths of 2500 m through the study of mass balance in a rectangular Box in the Bay of Bengal (Murty, 1990).

5. Conclusions

Depending upon the nature of forcing, the property distributions examined based on the near synoptic data collected in the Bay of Bengal during southwest monsoon season of 1984, enabled division of the Bay into northern (freshwater influenced), central (wind influenced) and southern (thermohaline driven) regions.

The region north of 15N and east of 89E is wholly influenced to depths 40–90 m by the freshwater influx from the shoreward boundary and its movement offshore. These waters believably maintain their identity in the upper layers by the anticyclonic flows in these regions.

Over the central region, the prevailing southwesterly winds lead to divergence (and hence upwelling) at subsurface (50–100 m) depths giving rise to cold waters along the axis (oriented in a SW-NE direction) of the positive curl. This leads to cyclonic circulation in this region.

The Indian Ocean monsoon drift current plays an important role on the dynamics and thermohaline structure of the waters of the Bay south of 15N. A warm, high salinity watermass advects at shallower depths (50–100 m) into the Bay up to 14N via the monsoon drift current. The northward flowing intense (40 cm/s) eastern boundary current west of 92E (west of the Nicobar Islands) is thermohaline driven (largely due to freshwaters in the east plausibly drawn either from the Andaman Sea or from Malacca strait) unlike the eastern boundary current systems of the other oceans which are wind driven. Broadly, the eastern boundary current of the Bay of Bengal could be likened to a mirror image of the western boundary current off Somalia during this season though the physical boundaries and the forcings leading to these

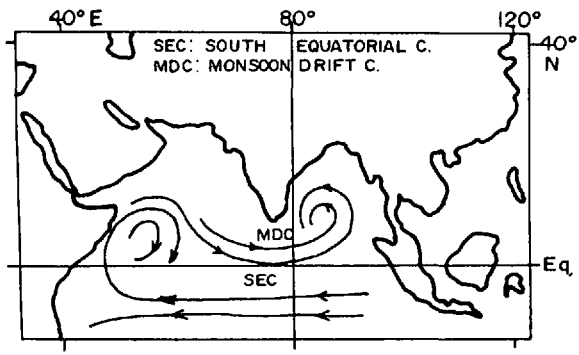

Figure 17. Schematic surface circulation in the Indian Ocean during southwest monsoon.

current systems differ significantly. While the South Equatorial Current (SEC) feeds the Somali current giving rise to an anticyclonic gyre in the Somali basin, the Monsoon Drift Current (MDC) feeds the large cyclonic gyre and partly supports an eastern boundary current in the Bay of Bengal (Fig. 17).

Further, the alternate ridge and trough structures in a SW-NE direction in the thermocline suggest the propagation of long period planetary waves from the southeastern Bay towards the western Bay. This is in line with the circulation modelling studies of the north Indian Ocean by Luther (1990) who pointed out the propagation of Rossby waves in the Bay of Bengal exited by the equatorial Kelvin waves in the southeastern Bay.

It is suggested that further studies are needed in this regard to understand the role of these waves on the circulation in the Bay.

Acknowledgments. The authors are grateful to Dr. B. N. Desai, Director for his keen interest in this study and Dr. J. S. Sastry, Head, Physical Oceanography Division for his useful comments on the paper. Thanks are also due to the anonymous referees for their critical evaluation and suggestions which improved the presentation and content of this article. Dr. J. C. Swallow has provided useful comments on the paper.

REFERENCES

Anon. 1954. Andhra University Memoirs in Oceanography. Vol. I, Andhra University Series 61, Andhra University, Waltair, 121 pp.

—— 1958. Andhra University Memoirs in Oceanography. Vol. II, Andhra University Series 62, Andhra University, Waltair, 237 pp.

—— 1968. Symposium on the Indian Ocean. Bulletin of National Institute of Sciences of India, 38, Part I, 552 pp.

Babu, M. T. 1987. Hydrography and circulation in the Bay of Bengal during post-monsoon season. M.Sc. Thesis. Bombay University, Bombay, India, 78 pp. (Unpublished).

Düing, W. 1970. The monsoon regime of the currents in the Indian Ocean. IIOE Oceanogr. Monograph, No. 1, East-West Centre Press, University of Hawaii, 68 pp.

Fomin, L. M. 1964. The Dynamical Method in Oceanography. Elsevier Oceanogr. Series, 212 pp.

Hastenrath, S. and P. J. Lamb. 1979a. Climatic Atlas of the Indian Ocean. Part II. Surface Heat Budget. University of Wisconsin Press, 93 charts.

—— 1979b. Climatic Atlas of the Indian Ocean. Part I. Surface Climatic and Atmospheric Circulation. University of Wisconsin Press, 97 charts.

Luther, M. 1990. Indian Ocean Modelling at the Florida State University, *in* Report of the 6th session of the CCCO Indian Ocean Climate Studies Panel held at Hawaii, U.S.A., SCOR-IOC/CCCO-IND-VI/3, Annex XII.

Mamayev, O. I. 1975. Temperature-Salinity Analysis of World Ocean waters. Elsevier Oceanography Series 11, New York, 374 pp.

Marchuk, G. I. and A. S. Sarkisyan. 1986. Mathematical Modelling of Ocean Circulation. Springer-Verlag, New York, 292 pp.

McCreary, J. 1990. Thermodynamics of the Arabian Sea, *in* Report of the 6th Session of CCCO Indian Ocean Climate Studies Panel, held at Hawaii, U.S.A., SCOR-IOC/CCCO-IND-VI/3, Annex XI.

Metcalf, W. G. 1968. Shallow currents along the northeastern coast of south America. J. Mar. Res., *26,* 232–243.

Molinari, R. L., D. Oslon and G. Reverdin. 1990. Surface current distributions in the tropical Indian Ocean derived from compilations of surface buoy trajectories. J. Geophys. Res., *95,* 7217–7238.

Murty, V. S. N. 1990. Some aspects of large scale circulation in the Bay of Bengal during southwest monsoon. Ph.D. Thesis. Submitted to the Andhra University, Waltair, India, 141 pp. (Unpublished).

Pond, S. and G. L. Pickard. 1983. Introductory Dynamic Oceanography. Pergamon Press, New York, 214 pp.

Ramasastry, A. A. and C. Balaramamurty. 1957. Thermal field and oceanic circulation along the east coast of India. Proc. Indian Acad. Sci., *46* section B, 293–323.

Ramasastry, A. A., M. R. M. Rao and N. C. Biswas. 1986. Cyclones and depressions over the Indian seas in 1984. Mausam, *37,* 1–8.

Rao, D. P. and J. S. Sastry. 1981. Circulation and distribution of some hydrographic properties during the late winter in the Bay of Bengal. Mahasagar-Bull. Natl. Inst. Oceanogr., *14,* 1–15.

Sastry, J. S., D. P. Rao, V. S. N. Murty, Y. V. B. Sarma, A. Suryanarana and M. T. Babu. 1985. Watermass structure in the Bay of Bengal. Mahasagar-Bull. Natl. Inst. Oceanogr., *18,* 155–162.

Sewell, R. B. S. 1925. Geographic and Oceanographic research in Indian Waters. Mem. Asiatic Soc. Bengal, *9,* 27–50.

—— 1932. Geographic and Oceanographic research in Indian waters: Temperature and Salinity of the deep waters of the Bay of Bengal and Andaman Sea. Mem. Asiatic Soc. Bengal, *9,* 357–423.

Suryanarayana, A., V. S. N. Murty and D. P. Rao. 1992. Hydrography and Circulation in the Bay of Bengal during early winter of 1983. Deep-Sea Res. (in press).

Sverdrup, H. U., M. W. Johnson and R. H. Fleming. 1942. The Oceans: Their Physics, Chemistry and General Biology. Prentice-Hall, New York, 1087 pp.

Varadachari, V. V. R. 1961. On the processes of upwelling and sinking on the east coast of India. Prof. Mahadevan Shastyabdapurti Commemoration Volume, Andhra University, Waltair, India, 159–162.

Varkey, M. J. 1986. Salt balance and mixing in the Bay of Bengal. Ph.D. Thesis. Kerala University, Kerala, India, 109 pp. (Unpublished).

Veronis, G. 1972. On properties of sea water defined by temperature, salinity and pressure. J. Mar. Res., *30,* 227–255.

Wyrtki, K. 1971. Oceanographic atlas of the International Indian Ocean Expedition. National Science Foundation, Washington, D.C., 531 pp.

—— 1973. Physical Oceanography of the Indian Ocean. In. Ecological studies. Analysis and synthesis. Vol. 3, B. Zeitzschel, ed., Springer-Verlag, Berlin, 18–36.

Received: *28 March, 1991;* revised: *17 March, 1992.*